Proc. Natl. Acad. Sci. USA
Vol. 92, pp. 9515–9519, October 1995
Neurobiology

G protein activation kinetics and spillover of γ-aminobutyric acid may account for differences between inhibitory responses in the hippocampus and thalamus

(synaptic transmission/neuromodulation/epilepsy)

ALAIN DESTEXHE*†‡ AND TERRENCE J. SEJNOWSKI*§

*The Howard Hughes Medical Institute, The Salk Institute for Biological Studies, Computational Neurobiology Laboratory, 10010 North Torrey Pines Road, La Jolla, CA 92037; †Department of Physiology, Laval University School of Medicine, Québec, QC Canada G1K 7P4; and §Department of Biology, University of California at San Diego, La Jolla, CA 92037

Communicated by Stephen Heinemann, The Salk Institute for Biological Studies, La Jolla, CA, June 14, 1995

ABSTRACT **We have developed a model of γ-aminobutyric acid (GABA)ergic synaptic transmission mediated by $GABA_A$ and $GABA_B$ receptors, including cooperativity in the guanine nucleotide binding protein (G protein) cascade mediating the activation of K^+ channels by $GABA_B$ receptors. If the binding of several G proteins is needed to activate the K^+ channels, then only a prolonged activation of $GABA_B$ receptors evoked detectable currents. This could occur if strong stimuli evoked release in adjacent terminals and the spillover resulted in prolonged activation of the receptors, leading to inhibitory responses similar to those observed in hippocampal slices. The same model also reproduced thalamic $GABA_B$ responses to high-frequency bursts of stimuli. In this case, prolonged activation of the receptors was due to high-frequency release conditions. This model provides insights into the function of $GABA_B$ receptors in normal and epileptic discharges.**

Two receptor types, $GABA_A$ and $GABA_B$, are responsible for most inhibitory postsynaptic potentials (IPSPs) mediated by the release of γ-aminobutyric acid (GABA) from presynaptic terminals. These receptors have characteristic differences in their kinetics (reviewed in refs. 1 and 2): $GABA_A$-mediated currents have a relatively fast time course (time constant, 5–20 ms), whereas $GABA_B$ receptors induce much slower changes in the excitability of the cell (time constant, 150–200 ms).

They differ as well in their activation. Typically, relatively strong stimulation is needed to evoke $GABA_B$ responses, whereas $GABA_A$-mediated currents are evoked even for very low levels of presynaptic stimulation. Miniature $GABA_A$ IPSPs also occur spontaneously and are thought to arise from the spontaneous release of GABA from a single vesicle, but they never have a $GABA_B$ component (2–4).

Physiological data on GABAergic responses show marked differences between thalamic and hippocampal slices. In the thalamus, stimulation of the reticular (RE) nucleus or interneurons induces biphasic GABAergic IPSPs in thalamocortical (TC) cells (5). The ratio between peak $GABA_A$ and $GABA_B$ currents evoked by RE neurons is insensitive to the intensity of the stimulation (6), but it changes markedly if the discharge of RE cells is enhanced by pharmacological means (6–9).

In hippocampal slices, GABAergic currents can be elicited in the dendrites of pyramidal cells by stimulating interneurons in the stratum radiatum. Unlike the situation in thalamic cells, the $GABA_A/GABA_B$ ratio depends critically on the intensity of the stimulation (10, 11) and on the presence of uptake (3, 12, 13).

The publication costs of this article were defrayed in part by page charge payment. This article must therefore be hereby marked "*advertisement*" in accordance with 18 U.S.C. §1734 solely to indicate this fact.

In this paper, we focus on the activation kinetics of $GABA_B$ responses, in which K^+ channels are activated through a guanine nucleotide binding protein (G protein) cascade (14, 15). We assume that this activation shows some "cooperativity," in the sense that independent binding of several G-protein subunits is needed to open the K^+ channels.

METHODS

Release, Diffusion, and Uptake of GABA. The equation for the diffusion of GABA in the synaptic cleft is

$$\frac{\partial T(\bar{x}, t)}{\partial t} = f_{\text{release}}(\bar{x}, t) - \frac{V_{\max} T(\bar{x}\, t)}{T(\bar{x}, t) + K_m} + D\nabla^2 T(\bar{x}, t), \quad [1]$$

where $T(\bar{x}, t)$ is the concentration of GABA at point $\bar{x}$ and time t, and the three terms on the right represent, respectively, release, uptake, and diffusion of GABA. The diffusion coefficient was $D = 8 \times 10^{-6}$ cm^2/s, based on values of compounds of similar molecular weight (16).

We simulated a two-dimensional array of square (0.5 × 0.5 μm) compartments (Fig. 1 *A* and *B*), representing the thin extracellular space between the postsynaptic neuron and processes emanating from other cells, either neurons or astrocytes. The area of each compartment was that of a typical single synaptic terminal (17); the array therefore represents many interleaved synaptic and glial terminals. The underlying assumptions are that (*i*) the width of the synaptic cleft [≈200 Å (17)] and extracellular space is less than the typical size of the synaptic terminal, allowing a two-dimensional approximation; (*ii*) the diffusion outside the area of terminals is negligible; (*iii*) the diffusion is instantaneous inside each compartment.

The release of GABA was simulated by increasing the concentration of GABA by 1 mM in the corresponding compartment when the presynaptic voltage crossed a threshold value of 0 mV. For a cleft width of 200–500 Å, a peak transmitter concentration of ≈1 mM (18) would correspond to 3000–7500 molecules of transmitter released (19).

Uptake, present in both interneurons and astrocytes (20), was modeled by a standard Michaelis–Menten equation, with a K_m value of 4 μM, estimated from kinetic studies of GABA transporters (21). The value of V_{max} could be only roughly estimated from the literature and was taken to be $V_{max} = 0.1$ M·s^{-1} in all compartments unless uptake was blocked.

In the absence of uptake, we modeled the slow decay of GABA in two ways: we simulated a large patch of postsynaptic membrane (900 μm^2) from which the transmitter leaked out

Abbreviations: GABA, γ-aminobutyric acid; IPSP, inhibitory postsynaptic potential; IPSC, inhibitory postsynaptic current; RE, thalamic reticular; TC, thalamocortical; G protein, guanine nucleotide binding protein.

‡To whom reprint requests should be sent at the † address.

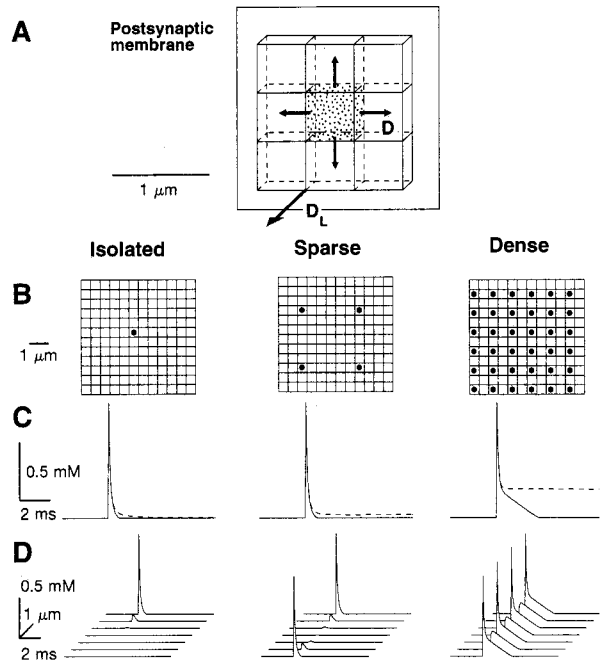

FIG. 1. Model of the release of transmitter at adjacent synapses in two-dimensional geometry. (*A*) Schematic representation of the model used with an array of adjacent processes (0.5 × 0.5 μm) representing interleaved synaptic terminals and astrocytes. Lateral diffusion (*D*) occurred in the extracellular space, with leakage to outside the membrane area (D_L). (*B*) Representation of three typical configurations: release in a single site (Isolated), release at a few sites simultaneously (Sparse), and high density of simultaneously releasing sites (Dense). (*C*) Time course of transmitter concentration at the release site represented with and without uptake (solid and dashed lines, respectively). (*D*) Time course of the transmitter represented for seven adjacent sites along a horizontal line in *B* in the presence of uptake.

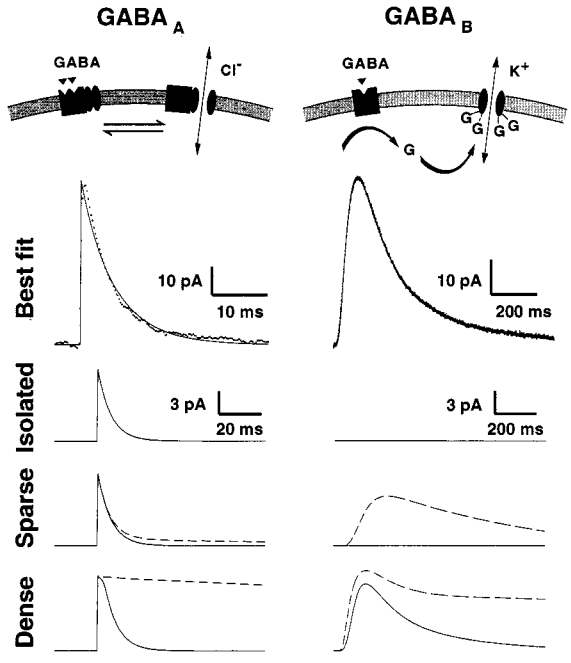

FIG. 2. Time course of GABAergic synaptic currents under different conditions. For each type of GABA receptor, $GABA_A$ (*Left*) and $GABA_B$ (*Right*), a schematic diagram is shown (*Top*) as well as the time course of the current under different conditions. Best fit: traces indicate the best fit obtained after running a simplex procedure to optimize the parameters (solid traces). Whole-cell-recorded GABAergic IPSCs were obtained from granule cells of the dentate gyrus (25, 26) (noisy traces; provided by T. Otis, Y. Dekoninck, and I. Mody). Traces below show GABAergic IPSCs at a single synapse for the three densities indicated in Fig. 1. Model IPSCs are shown in the presence (solid trace) and absence (dashed lines) of uptake.

only through the borders, neglecting diffusion in the third dimension. Alternatively, we introduced a leak in each compartment with a smaller diffusion coefficient ($D_L = 10^{-8}$ cm^2/s; see Fig. 1*A*). Both methods gave slow decay times comparable to that estimated from experiments (3, 13), but the latter was more convenient.

Integration of the reaction–diffusion equation (Eq. **1**) was performed using a first-order explicit integration method with a discretization step of $\Delta x = 0.5$ μm. The von Neumann criterion (see ref. 22) gives a minimal time step of $\Delta t = \Delta x^2/2D \simeq 150$ μs for numerical stability. We used $\Delta t = 10$–100 μs.

Binding of GABA on Postsynaptic Receptors. $GABA_A$ receptors have at least two binding sites for GABA and show desensitization (23, 24). However, blocking uptake reveals prolonged $GABA_A$ currents (3, 13), suggesting that desensitization was minimal. We neglected desensitization and modeled these receptors by using a simple first-order kinetic scheme (see ref. 27)

$$\frac{dr}{dt} = \alpha[T]^2(1 - r) - \beta r$$

$$I_{GABA_A} = \bar{g}_{GABA_A} r(V - E_{Cl}), \qquad [2]$$

where the binding of two molecules of transmitter T leads to the opening of the channel with rate constants of $\alpha = 2 \times 10^{10}$ $M^{-2}\cdot s^{-1}$ and $\beta = 162$ s^{-1} (obtained by fitting the model to whole-cell recorded $GABA_A$ current; Fig. 2 *Top Left*); the maximal conductance is $\bar{g}_{GABA_A} = 1$ nS, r is the fraction of receptor in the open state, and $E_{Cl} = -80$ mV is the chloride reversal potential.

The model of $GABA_B$ receptors was based on a model introduced previously (27), including a desensitized state of the receptor, several G-protein binding sites, assuming the G protein is in excess, and quasi-stationarity of the fast reactions

$$\frac{d[R]}{dt} = K_1[T](1 - [R] - [D]) - K_2[R] + K_3[D]$$

$$\frac{d[D]}{dt} = K_4[R] - K_3[D]$$

$$\frac{d[G]}{dt} = K_5[R] - K_6[G]$$

$$I_{GABA_B} = \bar{g}_{GABA_B}\frac{[G]^n}{[G]^n + K_d}(V - E_K), \qquad [3]$$

where $[R]$ and $[D]$ are, respectively, the fraction of activated and desensitized receptor, $[G]$ (μM) is the concentration of activated G protein, $\bar{g}GABA_B = 1$ nS is the maximal conductance of K^+ channels, $E_K = -95$ mV is the potassium reversal potential, and K_d is the dissociation constant of the binding of G on the K^+ channels. The G-protein cascade occurs in the following steps: (*i*) the transmitter binds to the receptor, leading to its activated form; (*ii*) the activated receptor catalyzes the activation of G proteins; (*iii*) G proteins bind to open K^+ channel, with n independent binding sites. Direct fitting of the model to whole-cell recorded $GABA_B$ currents gave the following values (Fig. 2 *Top Right*): $K_d = 100$ μM^n, $K_1 = 6.6 \times 10^5$ $M^{-1}\cdot s^{-1}$, $K_2 = 20$ s^{-1}, $K_3 = 5.3$ s^{-1}, $K_4 = 17$ s^{-1}, $K_5 = 8.3 \times 10^{-5}$ $M\cdot s^{-1}$, and $K_6 = 7.9$ s^{-1} with $n = 4$ binding sites (see *Results*). Some simulations were performed with $n = 1$ using different values of the parameters (not shown).

Estimation of Parameters. All simulations were run using NEURON (28). The values of parameters were obtained by fitting the entire model, including release, uptake, diffusion, and receptor kinetics, directly to experimental recordings with a simplex algorithm (22). At each iteration of the simplex algorithm, the model was run and the least-squares error was estimated between the experimental recording and the model. This procedure was repeated from different initial conditions to find robust values for the parameters, which were consistent with values estimated from the literature.

The values of the parameters were varied to test the sensitivity of the results; those that were critically important are explicitly discussed.

RESULTS

We first describe the time course of GABA in the synaptic cleft under different conditions and then show how this generates the observed GABAergic responses.

Time Course of GABA in the Synaptic Cleft. Fig. 1 *B–D* shows the three typical configurations considered here. In the first configuration, release occurred at an isolated site and GABA was present in the cleft extremely briefly (Fig. 1*C Left*), consistent with other models (18, 23, 29). GABA was practically undetectable 2 μm away from the release site (Fig. 1*D Left*). The decay of transmitter was biphasic with a fast initial decay governed by lateral diffusion (initial time constant, $\Delta x^2/4D \simeq 80$ μs) and a second slower component of low amplitude. The decay of the second component depended on the capacity (V_{max}) of GABA uptake and its time constant was $\approx$1.2 ms in the absence of uptake.

In the second configuration, GABA was released from sparsely spaced co-releasing sites and the time course of GABA in the cleft was nearly as brief as at an isolated site (Fig. 1 *C* and *D Center*). In the absence of uptake, the initial fast decay dominated by lateral diffusion was unchanged, but the slow component of decay was more prominent than at an isolated site.

In the third configuration, GABAergic terminals were densely packed (Fig. 1*B Right*) and although there was still a fast decaying phase due to lateral diffusion, the transmitter was prolonged. In the absence of uptake, the concentration of GABA stayed relatively high and decayed slowly everywhere (Fig. 1*C Right*).

For intermediate configurations, similar behavior was obtained over a wide range of geometries, values of the diffusion coefficient, and efficiency of uptake provided the density of co-releasing terminals was adjusted accordingly. The density of terminals was the critical factor.

Time Course of GABAergic Currents. The model was first adjusted to reproduce whole-cell-recorded $GABA_A$ currents (obtained from ref. 25). When a single release site was used, the kinetic model of $GABA_A$ receptors gave an excellent fit to $GABA_A$ currents recorded in hippocampal cells (Fig. 2 *Top Left*; parameters are given in *Methods*). For these values, release saturated the $GABA_A$ receptors (see refs. 1 and 2).

If there is more than one G-protein binding site, the activation of $GABA_B$-mediated currents is cooperative. Excellent fits to whole-cell-recorded $GABA_B$ currents in hippocampal cells were obtained for $n = 2$ or $n = 4$ G-protein binding sites (Fig. 2 *Top Right*).

We tested these kinetic models by using different densities of co-releasing terminals. For isolated GABA release, the $GABA_A$ current was insensitive to uptake and no $GABA_B$ current was evoked even if uptake was blocked (Fig. 2). For adjacent terminals with a low density, the time courses of both $GABA_A$ and $GABA_B$ inhibitory postsynaptic currents (IPSCs) were indistinguishable from isolated release if uptake was present ("Sparse" in Fig. 2). However, blocking uptake evoked a prolonged tail in the $GABA_A$ current, and a $GABA_B$ response could be revealed for a relatively narrow range of densities of releasing terminals. Finally, for high densities of simultaneously releasing sites, both $GABA_A$ and $GABA_B$ IPSCs occurred and their time courses were prolonged in the absence of uptake ("Dense" in Fig. 2).

Because of receptor saturation, $GABA_A$-mediated currents were relatively insensitive to the density of terminals and the exact time course of GABA; decay was dominated by the low value of the unbinding constant β. In comparison, the amplitude of $GABA_B$-mediated currents was highly sensitive to the time course of GABA in the cleft.

Intensity Dependence of GABAergic Currents. The dependence of the amplitude of the $GABA_B$ current evoked under normal conditions on the density of releasing sites is shown quantitatively in Fig. 3*A*, where a single release event was simulated with an increasing number of release sites. The total $GABA_A$ current increased linearly with the number of release sites, as predicted from Fig. 2. In contrast, $GABA_B$ responses appeared only for the strongest stimuli, corresponding to the highest densities of terminals.

$GABA_B$ responses also depended on the presynaptic pattern of activity. We investigated high-frequency trains of presynaptic action potentials (300 Hz) to mimic the frequency of bursting neurons in the thalamus. During high-frequency release at a single terminal, the time course of GABA during each individual release event was identical to that of isolated release (as in Fig. 1*C*). When increasingly long presynaptic bursts were delivered, $GABA_B$ responses were seen only for longer bursts (Fig. 3*B*).

The intensity dependence was highly influenced by the number of G-protein binding sites, n. A model with no

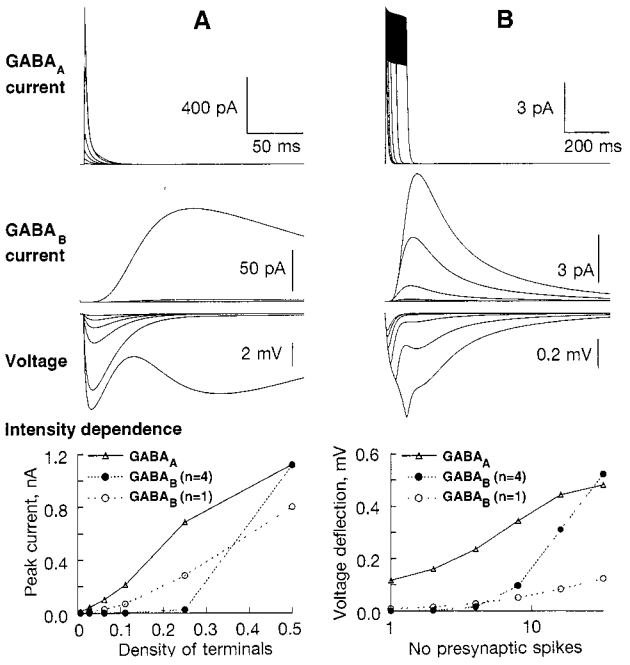

FIG. 3. Dependence of $GABA_A$- and $GABA_B$-mediated synaptic responses on the pattern of presynaptic stimulation. The $GABA_A$ current, the $GABA_B$ current, the postsynaptic potential, and the intensity dependence graph are arranged from top to bottom. (*A*) Dependence on the density of co-releasing terminals. Successive traces in each graph indicate the total postsynaptic current and voltage after a single presynaptic spike occurring simultaneously in 1, 4, 9, 16, 36, and 72 terminals (in a 144-compartment geometry). (*B*) Dependence on the number of presynaptic spikes occurring at a single synapse. In this case, the successive traces in each graph were obtained from trains of 1, 2, 4, 8, 16, and 32 presynaptic spikes at 300 Hz. (*Bottom*) Intensity dependence of $GABA_B$ responses are compared for single ($n = 1$) and multiple ($n = 4$) G-protein binding sites. $GABA_B$ current is scaled 10 times in *A*, and abscissa in *B* is in a logarithmic scale.

cooperativity (n = 1) was optimized identically as described above. In this case, $GABA_B$ responses were proportional to the stimulus (compare solid and open circles in Fig. 3 *Bottom*).

We simulated the properties of GABAergic responses in thalamic slices by using bursting models of RE cells based on the presence of a low-threshold calcium current (30) (Fig. 4*A*). Under normal conditions, stimulation in the RE nucleus evoked biphasic IPSPs in TC cells with a rather small $GABA_B$ component (Fig. 4*B*). We mimicked an increase of intensity by increasing the number of RE cells discharging. The ratio between $GABA_A$ and $GABA_B$ IPSPs was independent of the intensity of stimulation (Fig. 4*D*) but only if the density of GABAergic synapses on TC cells was low. Blocking $GABA_A$ receptors locally in the RE nucleus enhanced the burst discharge of these cells and evoked a more prominent $GABA_B$ component in TC cells (Fig. 4*C*).

Results similar to those shown in Fig. 4 were obtained in models where we assumed that each RE cell establishes a dense aggregate of four GABAergic terminals on TC cells, as suggested by morphological studies (31). However, terminals from different RE cells had to be located sufficiently distant from each other, so that there was minimal spillover between them.

DISCUSSION

Several hypotheses have been proposed for explaining the properties of $GABA_B$ responses (1, 2, 32): (*i*) a co-released factor is needed to activate $GABA_B$ receptors; (*ii*) $GABA_B$ receptors are located extrajunctionally; (*iii*) different populations of interneurons mediate $GABA_A$ and $GABA_B$ responses. We have proposed and tested an alternative hypothesis that this effect is due to properties of the receptors and second messengers involved in generating these responses.

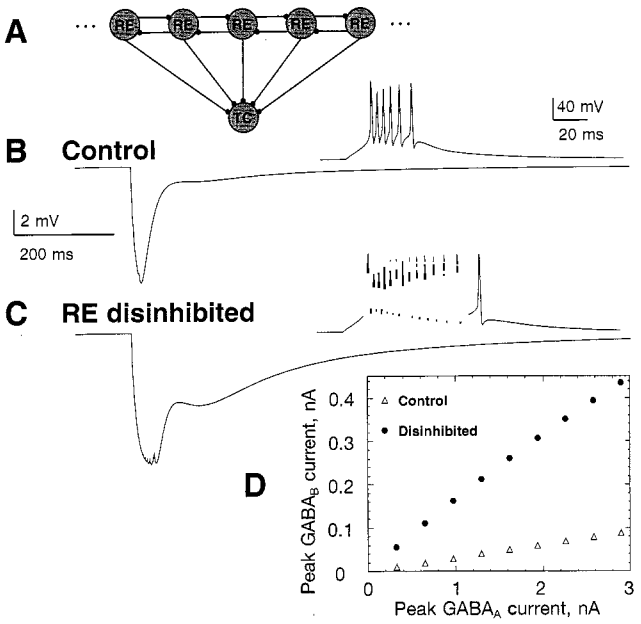

FIG. 4. Enhancement of the $GABA_B$ response in TC cells through disinhibition in the RE nucleus. (*A*) Connectivity: a simple network of RE cells was simulated with $GABA_A$ receptor-mediated synaptic interactions. All RE cells project to a single TC cell with synapses containing both $GABA_A$ and $GABA_B$ receptors. Models of the RE cells were taken from ref. 30. (*B*) In control conditions, the bursts generated in RE cells by stimulation have 2–8 spikes (*Inset*) and evoke in TC cells a $GABA_A$-dominated IPSP with a small $GABA_B$ component. (*C*) When $GABA_A$ receptors are suppressed in RE, the bursts become much larger (*Inset*) and evoke in TC cells a stronger $GABA_B$ component. (*D*) Peak $GABA_A$ versus peak $GABA_B$ current for increasing numbers of RE cells stimulated.

Time Course of GABA. Our model of the release of GABA included spillover from adjacent terminals and uptake in a two-dimensional extracellular space. Diffusion dominated the initial time course of transmitter decay, and uptake strongly limited the spillover to adjacent terminals, as proposed earlier (13). A more complete three-dimensional model would be needed to investigate these points in more detail.

The concentration of GABA was significantly influenced by the density of co-releasing terminals. We found a prolonged presence of GABA when many adjacent sites co-released, which was critical for $GABA_B$ responses.

Cooperativity of $GABA_B$ Responses. The multiplicity of G-protein binding sites assumed here had previously been suggested to explain the multiexponential time course of the $GABA_B$ current (26). In this paper, we showed that this hypothesis can also explain the characteristic properties of $GABA_B$ responses.

With several G-protein binding sites, a sufficient level of G protein must be activated intracellularly in order to produce a detectable K^+ current. This implies that prolonged activation of the receptors must occur to evoke $GABA_B$ responses. This property can account for the following observations: (*i*) $GABA_B$ currents can be revealed by facilitating transmitter release with sucrose (33). (*ii*) There is no $GABA_B$ component in miniature IPSCs (3, 4), in unitary IPSPs recorded from dual impalements (34), or in IPSPs obtained from very weak stimulation (13). These situations were simulated by the present model assuming that release occurred at single or distantly located sites. (*iii*) $GABA_B$ currents show multiexponential decay, a 10- to 20-ms delay of onset and a sigmoidal rising phase (26) (Fig. 2*B*). The delay was needed here for the active G protein to build up intracellularly to reach a level sufficient to activate the K^+ channels. Other potential mechanisms may also contribute (see ref. 15). (*iv*) Other models of $GABA_B$ transduction, including a more detailed model (27) and a simplified model with pulses of transmitter (unpublished data), produced very similar results only if there were multiple G-protein binding sites. The same conclusion has been reached independently in another model (D. Golomb, X. J. Wang, and J. Rinzel, personal communication).

Evoking $GABA_B$ Responses. We simulated the intensity dependence of GABAergic responses assuming that increasing stimulus intensities recruited more presynaptic neurons. If the terminals emanating from these neurons were densely packed, then significant spillover occurred. In this case, $GABA_A$ and $GABA_B$ components were evoked with a relative amplitude that depended on intensity, similar to observations in hippocampal slices (10, 11). In contrast, if the terminals were sparse, the $GABA_B$ component could be evoked only with high-frequency release. Such conditions arise when presynaptic neurons produce bursts of action potentials. In this case, the $GABA_A/GABA_B$ ratio was independent of the number of presynaptic neurons discharging, similar to observations in thalamic slices (6). Two factors were critical in determining $GABA_B$ responses: the density of co-releasing terminals and the number and frequency of presynaptic action potentials.

In hippocampal (35) and thalamic slices (5–7, 9), $GABA_B$ responses are often enhanced after the application of $GABA_A$ antagonists such as bicuculline. Several explanations have been proposed—for example, different populations of interneurons may mediate $GABA_A$ and $GABA_B$ responses (5) or there may be an enhanced action potential discharge due to an increase in synchrony and disinhibition of inhibitory neurons (6, 7, 9, 36). We propose that disinhibition alone provides the conditions for bicuculline-enhanced $GABA_B$ responses. If inhibitory neurons contact each other via $GABA_A$ receptors, then their discharges would be stronger after blockade of this inhibition. These enhanced discharges would then provide the stronger stimuli needed to fully evoke $GABA_B$ currents, as illustrated in Fig. 4.

Our model suggests that $GABA_B$ currents could help switch the thalamus from tonic to bursting mode. In awake animals, RE cells discharge single spikes tonically at a rate of 10–40 Hz, which evoke only fast IPSPs, in contrast to the biphasic IPSPs seen during sleep (37). In our model, RE cells elicited $GABA_B$ currents only when they were bursting. As $GABA_B$ IPSPs can powerfully promote bursting activity in TC cells (5), and TC bursts effectively evoke RE bursts (6, 9, 36, 37), $GABA_B$ currents may act as a "filter," transparent to tonic activity but strongly activated by bursting activity, serving to maintain the thalamus in a bursting mode. Petit mal epileptic discharges may be a perversion of this natural phenomenon through disinhibition in the RE nucleus (6, 7, 9, 36).

Testing the Hypothesis of G-Protein Cooperativity. The present model explains the differences between thalamic and hippocampal inhibitory responses, but it is also possible that there are regional differences in the distribution of GABAergic receptors or that different receptor subtypes are expressed in different regions.

The model makes several testable predictions. First, the predicted multiplicity of G-protein binding sites can be tested by applying activated G proteins on membrane patches (38) or by voltage-clamp experiments. In other systems, a tetrameric structure was demonstrated for the K^+ channels (15), and the kinetics of G-protein action were shown to involve several G-protein binding sites on the channel (39–41).

The second prediction is that $GABA_B$ responses are highly nonlinear (Fig. 3*B*). The sharp dependence of $GABA_B$ currents with an increasing number of presynaptic spikes could be verified by using dual impalements.

The third prediction is that there should be a higher density of dendritic GABAergic terminals in the hippocampus compared to the thalamus. GABAergic terminals are relatively dense on the dendrites of hippocampal cells (42), but precise measurements have not been made. In the thalamus, dense aggregates of a few inhibitory terminals have been observed on the dendrites of TC cells (31), but these aggregates were sparse and might originate from different presynaptic RE cells (E. G. Jones, personal communication), consistent with the present model.

We acknowledge Drs. T. Otis, Y. Dekoninck, and I. Mody for kindly providing access to their data; Drs. J. Clements and J. Huguenard for comments on the manuscript; and Dr. T. Bartol for insightful discussions. This research was supported by the Howard Hughes Medical Institute and the National Institutes of Health.

1. Mody, I., Dekoninck, Y., Otis, T. S. & Soltesz, I. (1994) *Trends Neurosci.* **17,** 517–525.
2. Thompson, S. M. (1994) *Prog. Neurobiol.* **42,** 575–609.
3. Thompson, S. M. & Gahwiler, B. H. (1992) *J. Neurophysiol.* **67,** 1698–1701.
4. Otis, T. S. & Mody, I. (1992) *J. Neurophysiol.* **67,** 227–235.
5. Soltesz, I. & Crunelli, V. (1992) *Prog. Brain Res.* **90,** 151–169.
6. Huguenard, J. R. & Prince, D. A. (1994) *J. Neurosci.* **14,** 5485–5502.
7. Huguenard, J. R. & Prince, D. A. (1994) *J. Neurophysiol.* **71,** 2576–2581.
8. von Krosigk, M., Bal, T. & McCormick, D. A. (1993) *Science* **261,** 361–364.
9. Bal, T., von Krosigk, M. & McCormick, D. A. (1995) *J. Physiol.* **483,** 641–663.
10. Dutar, P. & Nicoll, R. A. (1988) *Nature (London)* **332,** 156–158.
11. Davies, C. H., Davies, S. N. & Collingridge, G. L. (1990) *J. Physiol.* **424,** 513–531.
12. Solis, J. M. & Nicoll, R. A. (1992) *J. Neurosci.* **12,** 3466–3472.
13. Isaacson, J. S., Solis, J. M. & Nicoll, R. A. (1993) *Neuron* **10,** 165–175.
14. Dutar, P. & Nicoll, R. A. (1988) *Neuron* **1,** 585–591.
15. Hille, B. (1992) *Ionic Channels of Excitable Membranes* (Sinauer, Sunderland, MA).
16. Atkins, P. W. (1986) *Physical Chemistry* (Freeman, New York), 3rd Ed.
17. Harris, K. M. & Landis, D. M. (1986) *Neuroscience* **19,** 857–872.
18. Clements, J. D., Lester, R. A., Tong, G., Jahr, C. E. & Westbrook, G. L. (1992) *Science* **258,** 1498–1501.
19. Bartol, T. M. & Sejnowski, T. J. (1993) *Soc. Neurosci. Abstr.* **19,** 1515.
20. Hertz, L. (1979) *Prog. Neurobiol.* **13,** 277–323.
21. Clark, J. A. & Amara, S. G. (1994) *Mol. Pharmacol.* **46,** 550–557.
22. Press, W. H., Flannery, B. P., Teukolsky, S. A. & Vetterling, W. T. (1986) *Numerical Recipes: The Art of Scientific Computing* (Cambridge Univ. Press, Cambridge, MA).
23. Busch, C. & Sakmann, B. (1990) *Cold Spring Harbor Symp. Quant. Biol.* **55,** 69–80.
24. Celentano, J. J. & Wong, R. K. (1994) *Biophys. J.* **66,** 1039–1050.
25. Otis, T. S. & Mody, I. (1992) *Neuroscience* **49,** 13–32.
26. Otis, T. S., De Koninck, Y. & Mody, I. (1993) *J. Physiol.* **463,** 391–407.
27. Destexhe, A., Mainen, Z. & Sejnowski, T. J. (1994) *J. Comput. Neurosci.* **1,** 195–230.
28. Hines, M. (1989) *Int. J. Biomed. Comput.* **24,** 55–68.
29. Bartol, T. M., Land, B. R., Salpeter, E. E. & Salpeter, M. M. (1991) *Biophys. J.* **59,** 1290–1307.
30. Destexhe, A., Contreras, C., Sejnowski, T. J. & Steriade, M. (1994) *J. Neurophysiol.* **72,** 803–818.
31. Liu, X. B., Warren, R. A. & Jones, E. G. (1995) *J. Comp. Neurol.* **352,** 187–202.
32. Benardo, L. S. (1994) *J. Physiol.* **476,** 203–215.
33. Otis, T. S., De Koninck, Y. & Mody, I. (1992) *Pharmacol. Commun.* **2,** 75–83.
34. Miles, R. & Wong, R. K. S. (1984) *J. Physiol.* **356,** 97–113.
35. Newberry, N. R. & Nicoll, R. A. (1985) *J. Physiol.* **360,** 161–185.
36. Steriade, M., McCormick, D. A. & Sejnowski, T. J. (1993) *Science* **262,** 679–685.
37. Steriade, M. & Deschênes, M. (1984) *Brain Res. Rev.* **8,** 1–63.
38. VanDongen, A. M. J., Codina, J., Olate, J., Mattera, R., Joho, R., Birnbaumer, L. & Brown, A. M. (1988) *Science* **242,** 1433–1437.
39. Yamada, M., Jahangir, A., Hosoya, Y., Inanobe, A., Katada, T. & Kurachi, Y. (1993) *J. Biol. Chem.* **268,** 24551–24554.
40. Boland, L. M. & Bean, B. P. (1993) *J. Neurosci.* **13,** 516–533.
41. Golard, A. & Siegelbaum, S. A. (1993) *J. Neurosci.* **13,** 3884–3894.
42. Babb, T. L., Prectorius, J. K., Kupfer, W. R. & Brown, W. J. (1988) *J. Comp. Neurol.* **278,** 121–138.